F. Goulding

UCRL-20625 c.1
UC-4 Chemistry
TID-4500 (57th Ed.)

RECEIVED
LAWRENCE
RADIATION LABORATORY

DOCUMENTS SECTION

TRACE ELEMENT ANALYSIS BY X-RAY FLUORESCENCE

F. S. Goulding and J. M. Jaklevic

May 1971

AEC Contract No. W-7405-eng-48

TWO-WEEK LOAN COPY

This is a Library Circulating Copy which may be borrowed for two weeks. For a personal retention copy, call Tech. Info. Division, Ext. 5545

DISCLAIMER

This document was prepared as an account of work sponsored by the United States Government. While this document is believed to contain correct information, neither the United States Government nor any agency thereof, nor the Regents of the University of California, nor any of their employees, makes any warranty, express or implied, or assumes any legal responsibility for the accuracy, completeness, or usefulness of any information, apparatus, product, or process disclosed, or represents that its use would not infringe privately owned rights. Reference herein to any specific commercial product, process, or service by its trade name, trademark, manufacturer, or otherwise, does not necessarily constitute or imply its endorsement, recommendation, or favoring by the United States Government or any agency thereof, or the Regents of the University of California. The views and opinions of authors expressed herein do not necessarily state or reflect those of the United States Government or any agency thereof or the Regents of the University of California.

TRACE ELEMENT ANALYSIS BY X-RAY FLUORESCENCE

F. S. Goulding and J. M. Jaklevic
Lawrence Radiation Laboratory
University of California
Berkeley, California 94720

May 1971

ABSTRACT

The use of semiconductor detector X-ray fluorescence spectrometers for analysis of trace-element constituents of materials is described. The results presented illustrate the value of the technique in a wide variety of applications including analysis of food samples, biological specimens, and air filters. Levels of detection in these samples are less than 0.1 ppm. These results are achieved using X-ray excitation of the samples; they can therefore be achieved using only a small laboratory instrument and in a time measured only in minutes. Sample preparation is very simple compared with other techniques of comparable sensitivity.

FOREWORD

Recent months have been marked by a new public awareness of the adverse effects of trace elements in the air we breathe, in the water we drink, and in the food we eat. However, since many trace elements are known to be essential to life in its wide variety of forms, a better definition of the roles of trace elements, both adverse and desirable, in biological systems seems essential in the future. Further, a number of studies have shown the potential value of measurements of trace elements in blood and urine as an aid in the diagnosis of some diseases. These factors all point to the need for a measurement technique capable of rapid assessment of a broad range of trace elements present at very low levels (0.01 to 100 ppm) in all types of organic material.

We hope to show that X-ray fluorescence analysis using semiconductor detectors provides this tool. The account of the method and the early results presented here were the subject of a talk recently at the Lawrence Radiation Laboratory (Berkeley), where many of the significant advances in this field were made. The work provides one illustration of the value of nuclear research in developing techniques having broad applications to the problems of society.

I. PHYSICS OF THE X-RAY FLUORESCENCE METHOD

Every scientist is familiar with the brilliant yellow sodium light produced when salt falls into a flame, and with the fact that our knowledge of the constitution of stars derives from studies of the light they emit. Optical spectroscopy, thanks to our fine natural light detectors, and also to Newton's use of prisms to disperse light according to its color, is now a commonplace tool in chemical analysis. However, a casual observer is overwhelmed by the complexity of optical spectra, caused mostly by the abundance of levels in the outer shells of atoms involved in light production. By observing X rays, we can do elemental analysis much more easily, for the inner-atomic-shell structure producing X-rays is quite simple, and only a few X-ray wavelengths are emitted. X-ray spectroscopy requires both detection of X-rays and measurement of their energy; both functions are performed conveniently and well by semiconductor detectors--hence the power of these devices as analytical tools.

The simple design of a semiconductor X-ray fluorescence spectrometer is shown in Fig. 1; the physical mechanisms involved in the fluorescence process are also illustrated. Spectroscopy of photoelectrons and Auger electrons can also be used for analysis purposes, and the outstanding energy resolution of electron spectrometers permits measurement of changes in energy levels due to chemical-bonding effects. However, the short range of electrons in materials limits the use of electrons--compared with X-ray--spectroscopy. A wide range of methods of exciting characteristic X rays is available. We discuss here only X-ray excitation of the sample, as our objective is to

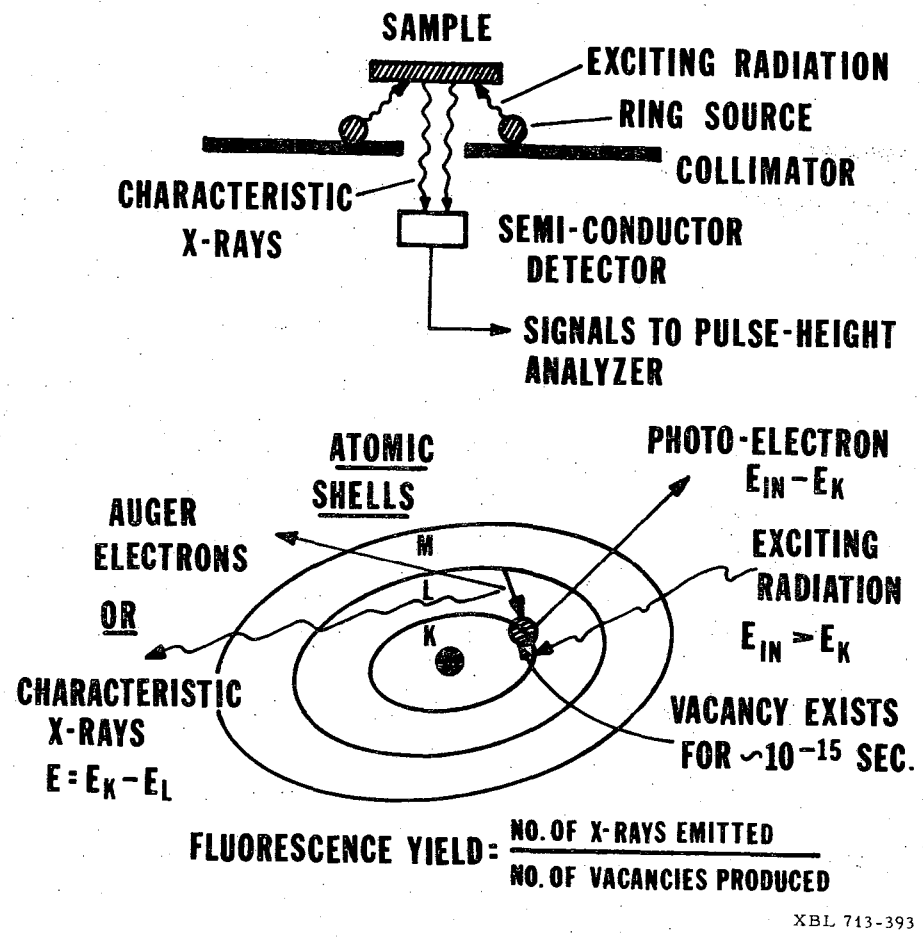

XBL 713-393

Fig. 1. Basic X-ray fluorescence spectrometer and the atomic processes.

illustrate a relatively simple instrument; other, more complex, methods of excitation may be employed and are favoured for some purposes.

The atomic-shell transitions generating the X-rays of interest in this paper are shown in Fig. 2. In the energy range of interest here, the energy resolution of semiconductor-detector spectrometers is such that the $K\alpha_1$ and $K\alpha_2$ lines are observed as a single line, as are the ($K\beta_1$, $K\beta_2$) and the ($L\beta_1$, $L\beta_2$, $L\beta_3$) lines. The intensity of the $K\beta$ peak is always much smaller than that of the $K\alpha$ line, while the $L\alpha$, and $L\beta$ lines are of similar intensity to each other, and are large compared with the other L X-rays.

Energies of primary interest lie below 30 keV, where the K X-rays of elements with $Z < 55$ are observed, and the L X-rays of the heavy elements also appear. Figure 3 shows the energies of these X-rays. The L X-ray energy of a heavy element may be the same as the K X-ray energy of a light element causing confusion in analysis; but heavy elements are relatively rare in biological material, so the resulting problem is of less importance in practice than perhaps might be expected. Often, the presence of two strong L lines is useful--for example, Pb $L\alpha$ coincides with the common As $K\beta$, but Pb $L\beta$ only clashes with Kr, an uncommon contaminant. This fact permits determination of lead even when arsenic is present.

As shown in Fig. 1, Auger-electron emission provides an alternative method of filling vacancies in the atomic shells, thereby reducing the yield of fluorescent X-rays. Unfortunately, the emission of Auger electrons becomes highly probable for low-energy transions, so the fluorescent yield becomes very small for light elements, as shown in

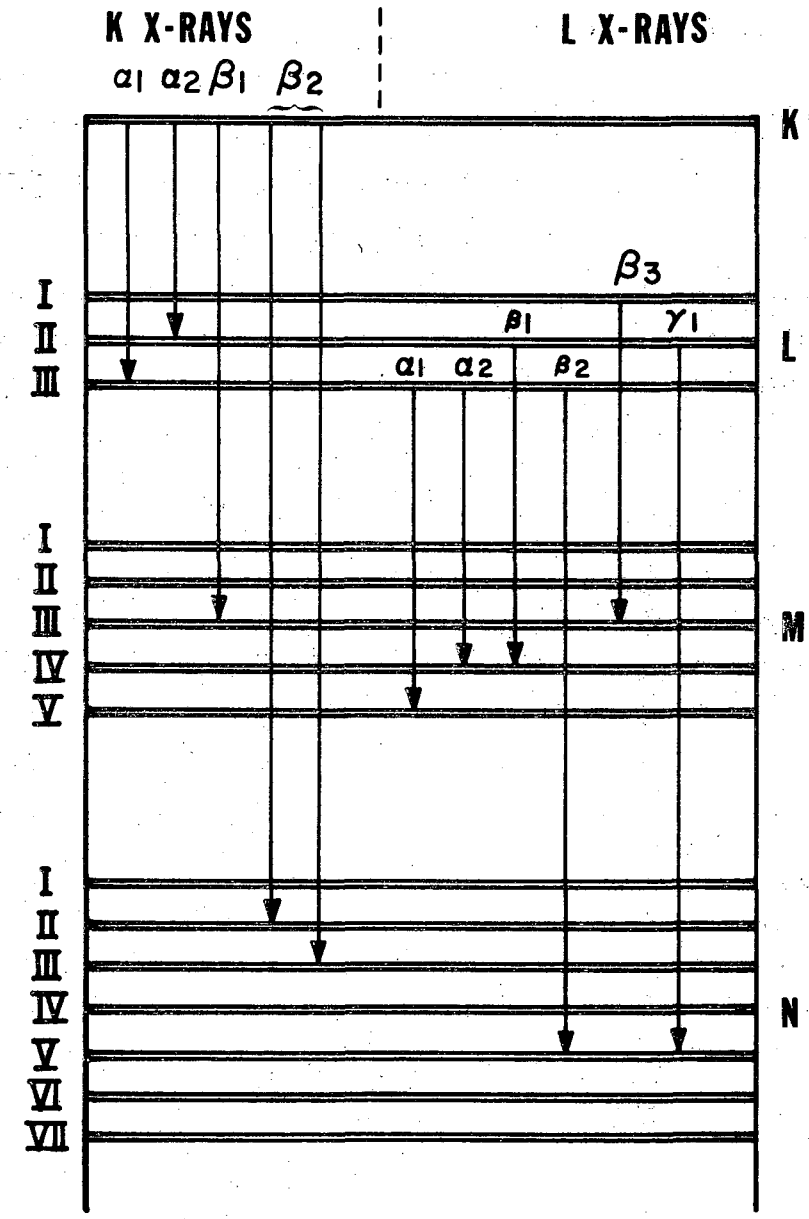

XBL 713-394

Fig. 2. Atomic energy levels involved in the emission of X-rays of interest in this paper.

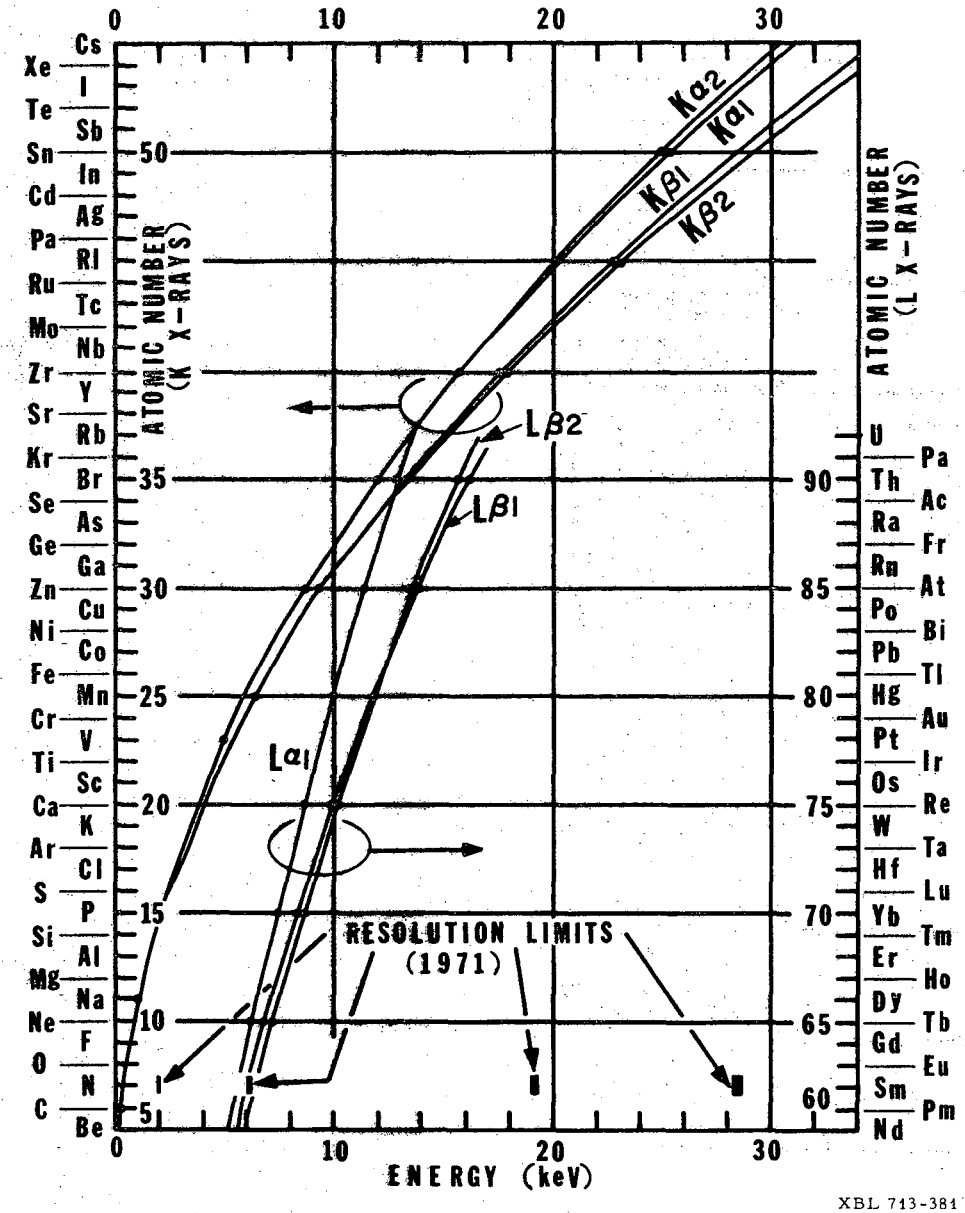

Fig. 3. Energies of K and L X-rays up to 30 keV.

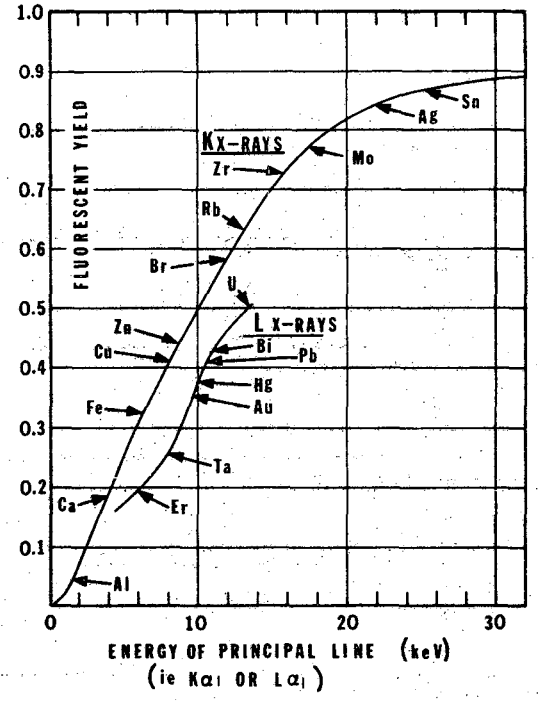

Fig. 4. Variation of fluorescent yield with energy for K and L X-rays.

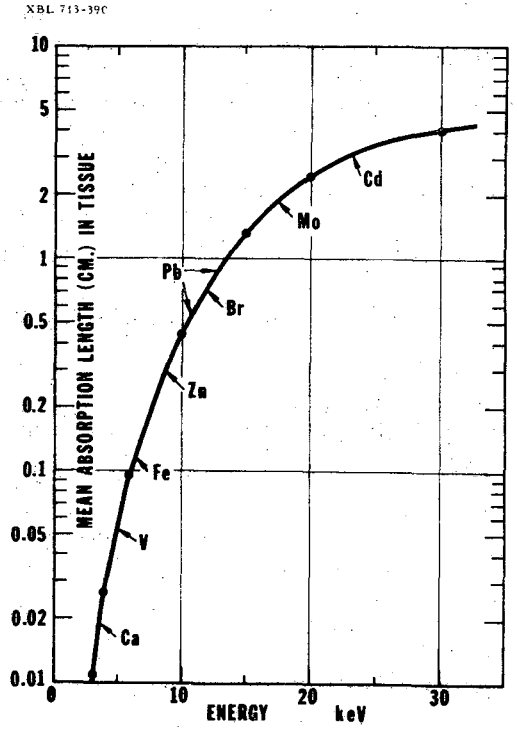

Fig. 5. Absorption length of X-rays in typical organic material as a function of energy.

Fig. 4. A similar behaviour is seen for L X-rays emitted by heavy elements. The low-fluorescent yield makes X-ray fluorescence spectrometers less sensitive for light elements; the problem is further exaggerated by the self-absorption of the fluorescent X rays in the sample itself. This factor restricts analysis to a vanishingly small surface layer of the sample for low-Z elements. Figure 5 shows the thickness of typical organic material required to attenuate different X-rays by a factor of 1/e--this curve shows that samples less than 1 mm thick must be used to avoid severe attenuation even of elements as high as iron in the periodic table.

Two further efficiency factors are important in the design of an X-ray spectrometer. The efficiency of any detector falls at high energies causing a loss of counts. Lithium-drifted silicon detectors 5 mm thick were used in these studies; so their efficiency is essentially unity in the energy range of interest here. Choosing the energy of the exciting radiation is a major step in the design of an X-ray fluorescence experiment; the probability of creating a vacancy is a maximum when the energy of the exciting radiation just exceeds the binding energy of the atomic shell involved. Figure 6 shows how the probability of vacancy creation in the K and L shells of various atoms depends on the energy of the exciting radiation. As an example of the use of these data, consider the case of a sample containing equal parts by weight of lead and bromine excited by Mo Kα radiation (17.4 keV). The lead L-shell vacancies will be excited 3.5 times as efficiently as the bromine K-shell vacancies; but since lead atoms are three times

as heavy as bromine, only one-third as many lead atoms are present. Moreover, the fluorescent yield for Pb L X-rays is about 25% less than that for Br K X-rays (Fig. 4). The total number of lead X-rays from the sample will therefore be slightly smaller than that of bromine K X-rays.

We have so far considered only the fluorescent X-rays produced in the sample, their excitation and transmission to the detector, and their absorption in the detector. The main mechanism for absorption in the detector in this energy range is the photoelectric process; even where Compton scattering occurs in the detector, the scattered photon will nearly always be absorbed photoelectrically to produce a total charge in the detector proportional to the total energy of the original incoming X-ray. This situation is a pleasant contrast to the dominance of the Compton effect in spectra observed when detecting higher-energy γ-rays. However, scattering processes are still a major factor in X-ray fluorescence spectroscopy--this time due to the effect of scattered radiation from the sample into the detector. Both coherent (elastic) and incoherent (Compton) scattering from the sample matrix, the organic base containing the trace elements, are present, the relative proportions depending on the ratio of light to heavy nuclei present. Figure 7 shows the energy exchanges involved in Compton scattering at these energies. Even 180°-scattering of 20-keV photons involves a loss of energy of only about 1.5 keV to the photon involved in the scattering process.

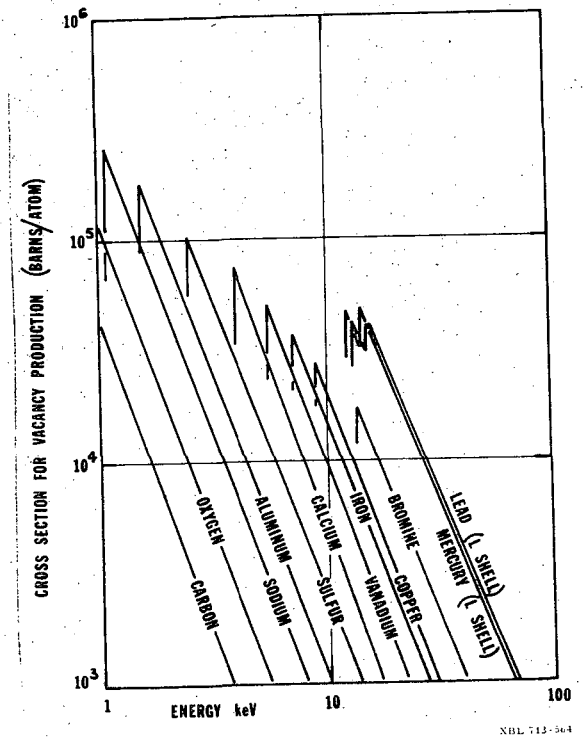

Fig. 6. Cross section for K- (or L-) shell vacancy formation in several elements as a function of energy.

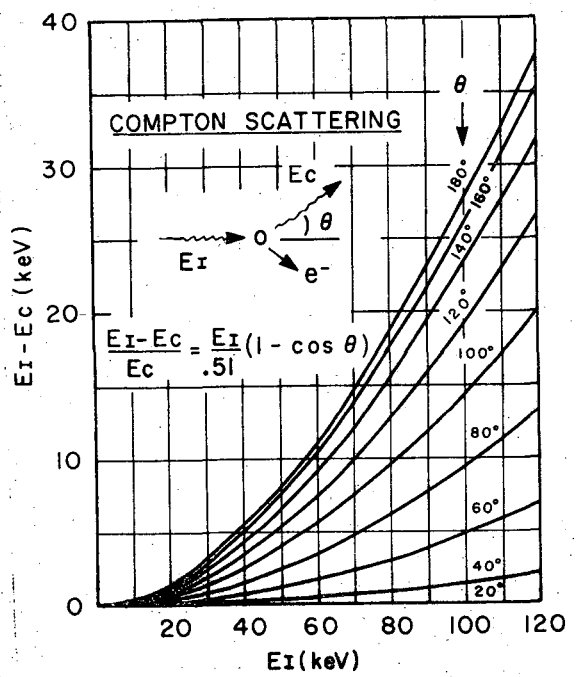

Fig. 7. Energetics of the Compton-scattering process at energies below 120 keV.

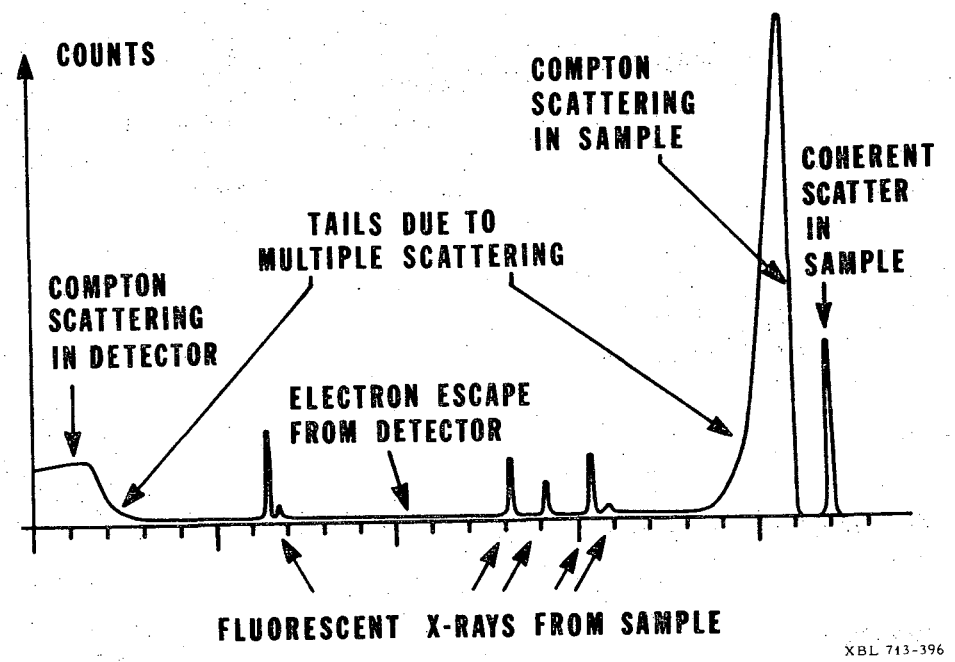

Fig. 8. Idealized spectrum observed by an X-ray fluorescence spectrometer.

We are now in a position to appreciate the general form of the spectrum (Fig. 8) observed by a X-ray fluorescence spectrometer. The dominant feature of the spectrum is the large scatter peaks that may constitute 99% of the total counts observed. At the very-low-energy end of the spectrum we see the effect of scattered photons from the sample which happen to Compton-scatter from electrons in the detector and escape, leaving only the knock-on electron energy in the detector. The central region of the spectrum contains the interesting information on fluorescent X rays emitted by the sample--unfortunately superimposed on a background that, in an ideal case, is due only to photoelectrons from the detector escaping from its surface. Since the photons producing these electrons are primarily those scattered from the sample, and only part of the photon energy is converted into ionization in the detector, a continuum of pulse heights below the scatter peaks is generated by this process. As we will see later, other processes in the detector degrade events that should appear in the scatter peaks, resulting in increased background in the region of interest, thereby limiting our ability to see minute trace of impurities. The results given in this paper are made possible only by the methods of background reduction described herein.

The validity of this general picture is illustrated in an X-ray fluorescence spectrum obtained recently, shown in Fig. 9. The large incoherent scatter peak is shown, while the coherent scatter peak is just beyond the right margin of the figure. The Compton edge due to the detector, which would normally appear at the left of this figure,

has been removed by a discriminator in the electronic pulse pile-up rejection system employed in this experiment. The background level seen in this figure, while low, is at least ten times as high as can be explained by photoelectrons escaping from the detector surface.

For comparison, Fig. 10 shows the same sample examined by an X-ray fluorescence system with performance equal to units available in early 1965. The contrast between Figs. 9 and 10 is striking. In the next section of this paper, an account will be given of the major steps taken in the past five years that account for the vast difference between these two results.

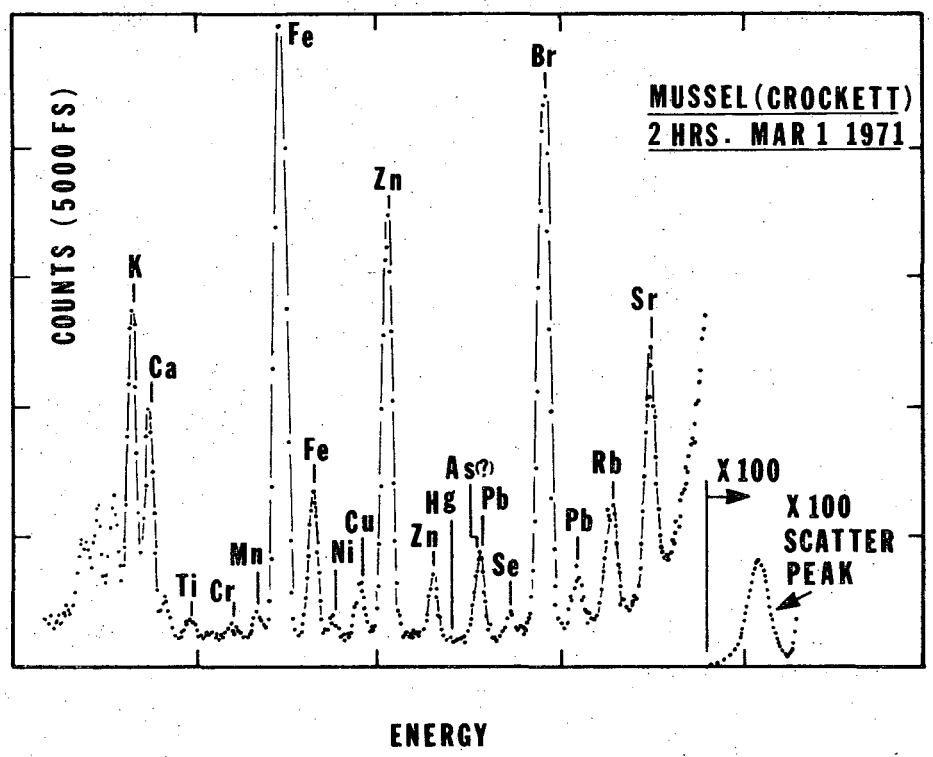

XBL 713-384

Fig. 9. A practical spectrum obtained with Mo X-ray excitation of a freeze-dried Mussel sample. This measurement used a modern high-resolution spectrometer containing a guard-ring detector (see section II B).

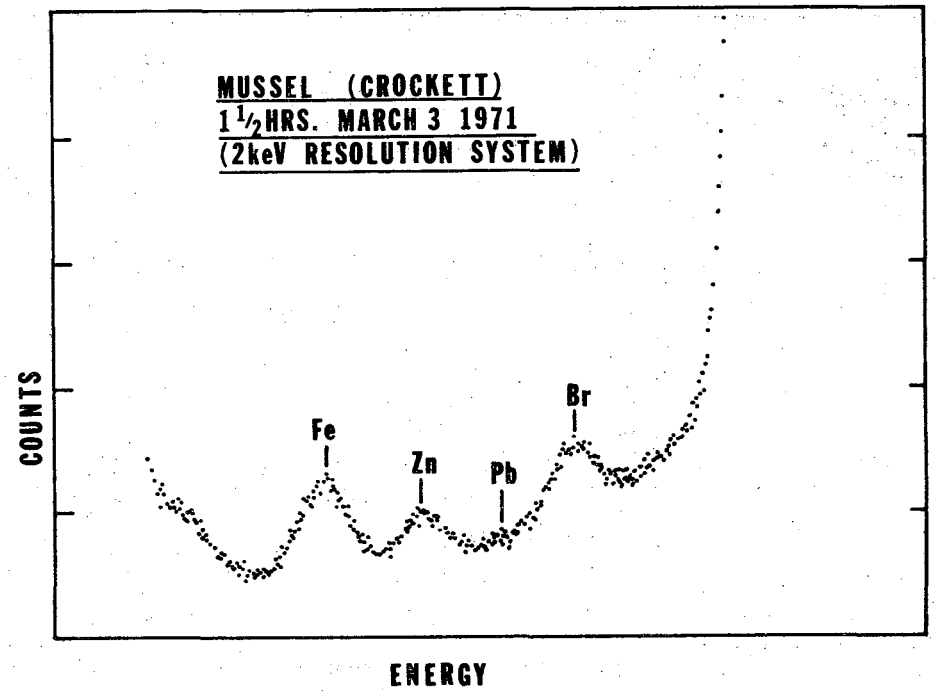

XBL 713-403

Fig. 10. Spectrum obtained with the same sample as Fig. 9 but using a system typical of the state-of-the art in 1964.

BLANK

BLANK

II. DEVELOPMENT OF THE INSTRUMENT

The developments of the past few years that resulted in this new analytical technique have involved improvements in the electronics of semiconductor detector spectrometers to improve energy-resolution and high-counting-rate behaviour; detector developments to reduce or eliminate undesirable background; and development of small X-ray tubes that can be used as intense sources of nearly monoenergetic radiation to excite the sample, thereby speeding analysis by almost two orders of magnitude as compared with using convenient radioactive sources. We will briefly discuss each of these major areas of development.

A. Improving Electronics

The first major step toward improving energy resolution below 2 keV full-width at half maximum (FWHM) resolution, the level common in 1964, came with the development of low-noise field-effect transistors by a number of transistor manufacturers. Earlier field-effect transistors exhibited considerable surface noise, and their performance was not superior to the vacuum tubes commonly used in earlier preamplifiers. Following the development of a new generation of FET's (notably the 2N3823, then the 2N4416), low-temperature operation of these devices to reduce noise was introduced by a number of groups. Work at the Lawrence Radiation Laboratory (Berkeley) in mid-1965[1] achieved an energy resolution of 700 eV (FWHM), and stimulated the first suggestion[2] that a semiconductor detector spectrometer could provide a useful X-ray fluorescence analyzer. As can be seen in Fig. 3,

700-eV resolution permits separation of elements higher than zinc in the periodic table. Substantial improvements were necessary before general applicationsof the technique became possible.

A long slow period of development followed this initial jump in performance. Small improvements resulted from use of the 2N4416 to replace the 2N3823, from rigorous selection of these transistors, and from optimization of the operating temperature of the field-effect transistor. Changes in manufacturing techniques led to some improvement, but also some setbacks. By early 1969, a few outstanding spectrometers were capable of achieving energy resolutions as low as 250 eV (FWHM) at low energies, making separation of elements above calcium practicable.

Before these achievements, the energy resolution of an X-ray spectrometer for low-energy X-rays (say 10 keV) had been dominated by the electronic-noise contribution of the first amplifying device in the preamplifier. However, as shown in Fig. 11, statistical fluctuations in charge production[3] in the detector become increasingly important as the electronic noise is reduced.

A series of advances made at LRL over the past two years and illustrated in Fig. 12 have reduced the energy resolution of X-ray spectrometers to 100 eV or less, making possible the separation of all elements above carbon in the periodic table. The resistor, traditionally used to provide low-frequency feedback to a low-noise preamplifier as shown in Fig. 12A, was replaced by light coupling, from a light-emitting diode (LED) to the photosensitive drain-gate FET junction (Fig. 12B)[4]. This step eliminated the feedback

resistor, a noisy and unreliable component; it also entailed remounting the small FET silicon chip in a new package, thereby eliminating noise produced by the FET header. The elimination of these noise sources permits use of longer pulse-shaping times in the main amplifier* thereby achieving energy resolution below 100 eV at low counting rates. In this simple light feedback system, nonlinearity of the LED current-light relationship degraded performance at higher counting rates. This led to the pulsed-light feedback scheme shown in Fig. 12C[5]. Here the LED is pulsed when necessary to maintain the preamplifier output in its normal range. When pulsing occurs, a reject waveform is fed to the main amplifier, and all signals are rejected until the system resumes normal operation.

The simplified diagram of the amplifier system used in the pulsed-light feedback unit, shown in Fig. 13, gives some idea of the complex processing performed on signals before they are allowed to proceed to a pulse-height analyzer. Signals from the preamplifier are differentiated, shaped, and amplified in a linear amplifier, then fed to a circuit that accurately fixes the baseline of the signals at zero. The action of this restorer is inhibited during the reset action in the preamplifier. A fast channel also processes the signals, looking for cases where pile-up occurs in the slow channel--in which case the events are rejected. If no pile-up occurs, the signal in the slow

* Nuclear pulse amplifiers include pulse-shaping networks containing differentiators and integrators to optimize the system signal-to-noise ratio.

channel is examined; and if its level exceeds a selected bias level, the signal peak is stretched. Shortly after the signal peak, the stretched output is sampled by a linear gate, and a 2 μs-wide output signal, proportional in amplitude to the difference between the signal and the selected bias, is produced. It is an impressive demonstration of the power of modern integrated circuits that these functions--amplification, shaping, pile-up rejection, dc restoration, gating, signal stretching and biased amplification--are performed in a single small module (NIM-2 width). The performance is equally impressive, as seen in Fig. 14 where the behaviour of an X-ray spectrometer analyzing the Mn X-rays produced by an ^{55}Fe source is shown. The total input counting-rate was 260,000 counts/sec; double, triple, and even quadruple pile-ups, within the 0.15-μs resolving time of the pile-up rejection circuitry, are clearly resolved.

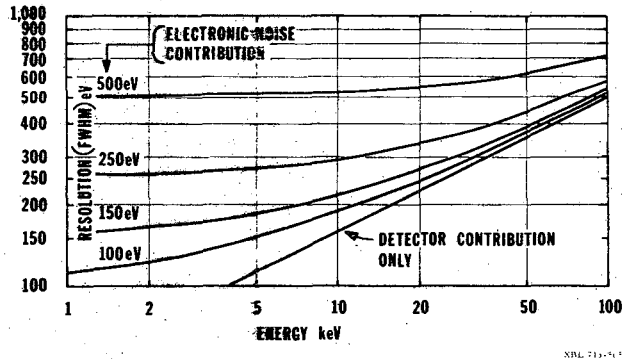

Fig. 11. The energy resolution of a spectrometer as a function of electronic noise and detector charge-production statistics.

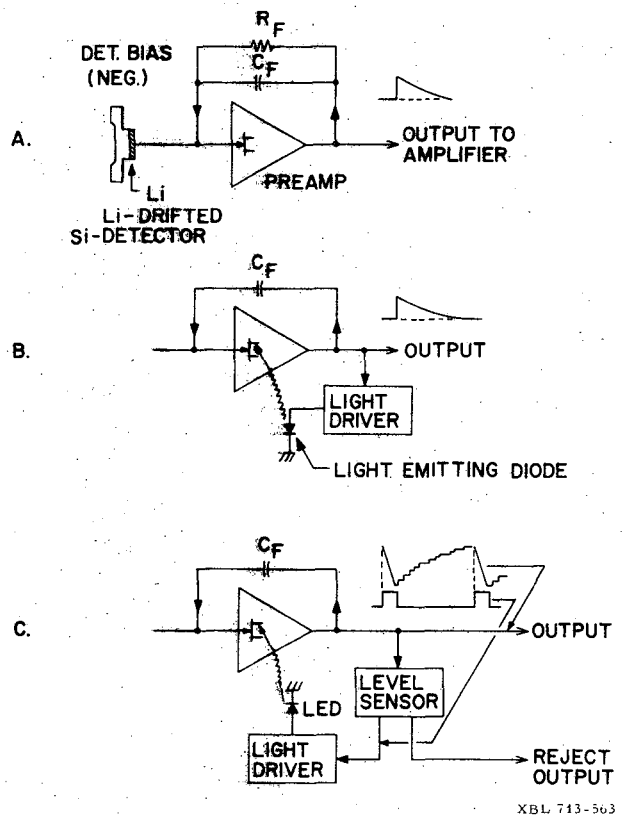

Fig. 12. Development of pulsed-light feedback preamplifier from a resistor feedback configuration.

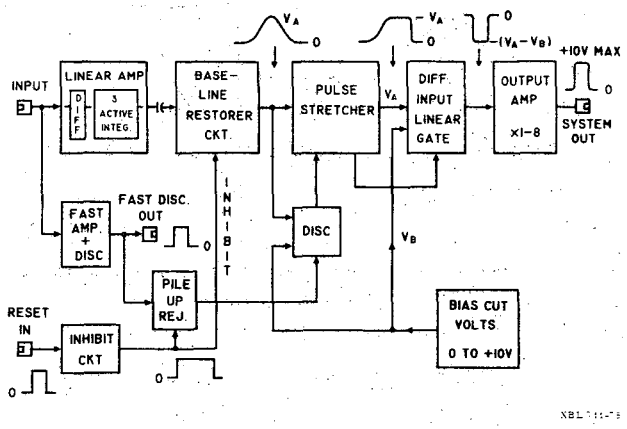

Fig. 13. Block diagram of the amplifier unit used with a pulsed-light feedback system.

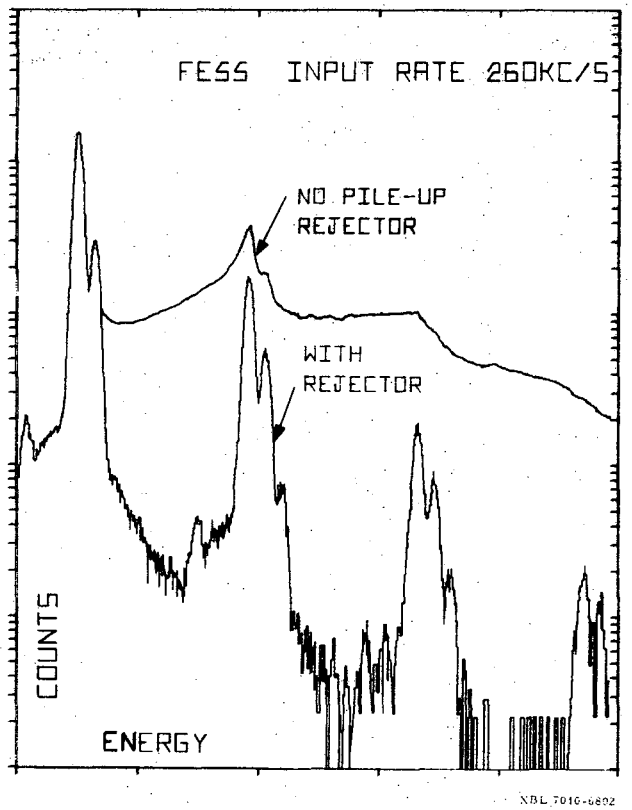

Fig. 14. High-rate performance of the pulsed-light feedback system.

B. Reducing Detector Background

Only a few of the X-rays reaching the detector are characteristic X-rays from the trace elements in the specimen--the rest are backscattered either coherently or incoherently from the matrix of the sample. Since Compton scattering of X-rays by electrons in the sample degrades the photon energy by only a small amount (see Fig. 7), the backscattered X-rays have energies close to that of the exciting photons, and higher than the characteristic X-rays of the elements of interest in the spectrum. This situation was illustrated in Fig. 8, which also shows the background resulting from degraded signals produced by a few of the high-energy scattered photons. Since this background sets the limit to the ability of the spectrometer to detect minute quantities of trace elements, its reduction is one of our most important problems.

The background arises from a number of sources, all resulting in a smaller electrical signal than should be produced by the photon incident on the detector:

i) Escape of the characteristic K X-ray of the detector material from the sensitive volume. The K X-rays of silicon are of low energy (1.74 keV), so very few escape (about 0.1%). The main result is a slight increase in the low-energy tail on the scatter peak. Escape is a more important problem in germanium detectors (K X-ray energy = 9.88 keV), as will be shown in a later figure.

ii) Escape of the photon-induced photoelectron from the surface of the detector. In this case, only part of the electron's energy generates ionization in the detector, so the electrical signal is smaller than should be produced. Typically, the contribution to background by this mechanism should be very small (< 1% of the scatter-peak counts, and this fraction should decrease when the scatter-peak energy is increased. In practice, the background in fluorescence spectra increases rapidly as the energy of the scatter peak increases, indicating that electron escape is not the primary source of background.

iii) Escape of degraded photons following single Compton collisions with electrons in the detector. The probability of Compton collisions is very small at these energies compared with that of photoelectric processes. Multiple collisions followed by escape would produce signals in the main range of interest in fluorescence spectra, but this combination is very improbable. The very low-energy region of a spectrum is the only part affected by the Compton escape process.

iv) Defects on the charge-collection process in the detector that result in loss of some of the charge produced by the incident photon. Our recent work has shown that this has been the major source of background in earlier semiconductor detector X-ray spectrometers, and its reduction is the key development making possible trace element analysis.

We have now identified the major source of detector background as being due to charge loss in the side surfaces of the detector. One of the commonest types of detector geometry (the "top-hat") is shown in the first illustration of Fig. 15. The electric field is normally considered to be perpendicular to the lithium and gold faces, but distortion of the electrical field occurs due to the non-neutral electrical behaviour of the side surfaces. Typical detectors are 3 or 5 mm thick, with a 5-mm diameter top-hat having a rim only about 1 mm thick--these dimensions represent a compromise between the effects of detector capacity on energy resolution of the system, and X-ray efficiency considerations. Some of the charge produced by photons incident away from the center of the detector flows in the surface layers, and is only partially collected. The resulting degraded pulses produce background as seen in the upper curve of Fig. 15. Here, Te X-rays (27 keV) were incident on the detector, and almost 40% of the total events appeared in the background below the main peak.

We have devised the guard-ring detector shown in the second illustration in Fig. 15 to reduce this background. Here the central sensitive region of the detector is surrounded by an annular guard ring whose purpose is to define the charge collection region by internal electric field lines, rather than by surfaces of unknown character. The success of the method is illustrated by the lower curve in Fig. 15.

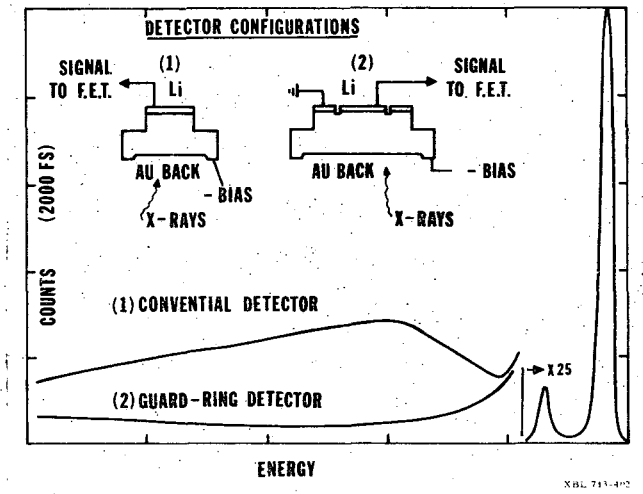

Fig. 15. Background behaviour of conventional and guard-ring detectors.

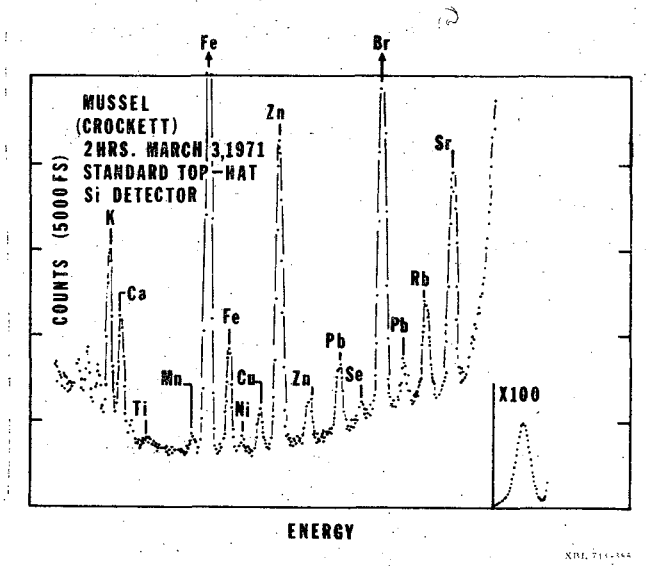

Fig. 16. Performance of a system using a conventional detector on the same sample as shown in Fig. 9.

The background is reduced by a factor of almost 10 compared with the conventional detector, so that only about 6% of the total counts now appear in the background. While this is far from the background we expect from electron escape, and further work remains to be done*, the reduced background gives a substantial improvement in the performance of X-ray spectrometers for trace analysis. A typical analysis using the guard-ring detector was shown in Fig. 9, while Fig. 16 shows the same specimen analyzed by a conventional detector. The difference in background is evident in this result.

It is interesting at this point to compare the performance of a germanium detector X-ray spectrometer with that of silicon. In Fig. 17, the spectrum obtained with a germanium detector is shown for the same sample as was used to give Fig. 9. We see that the peaks produced by the trace elements are largely obscured in the germanium case by various artifacts due to the detector itself. On the basis of this result, it appears that germanium detectors have little value for trace element analysis--at least in this energy range.

---

* Further work has been done, and the results appear in the Appendix to this paper. Apart from the results given in the Appendix, the results presented in this paper were all obtained with the guard ring used as in Fig. 15.

Apart from the generally flat background due to the detector, another type of background can exist in X-ray spectrometers, and must be recognized or eliminated if correct interpretations of spectral features are to be made. This background is due to fluorescence of trace elements in the collimators or detector used in the spectrometer, which are excited by the scattered photons from the sample. Figure 18 illustrates the nature of the background in a typical system irradiated with Zr X-rays. Several of the peaks observed (Fe, Cu, Zn) can be attributed to impurities in the Mo collimators used in the experiment. However, the two peaks in the vicinity of the Au L X-ray lines are of special importance due to their proximity to the normal location of Hg L X-ray lines. Since mercury is of particular importance in trace-element analysis, the situation shown in Fig. 18 is particularly unfortunate. Figure 19 shows the confusion caused by this problem in the analysis of a dried potato sample where the region of the Hg peaks appears to contain diffuse structure that defies analysis.

The source of this problem is now known to be the very thin (~200 Å) gold surface barrier present on the entry side of the detector. Fluorescence of the gold produces characteristic Au X-rays, but photoelectrons and Auger electrons, coincident in time with the X-rays, are also produced. Since the gold is in direct contact with the sensitive volume of the detector, some of the energy of these electrons may be deposited in the sensitive region of the detector, adding to the X-ray signal. Close examination of Fig. 18 shows that

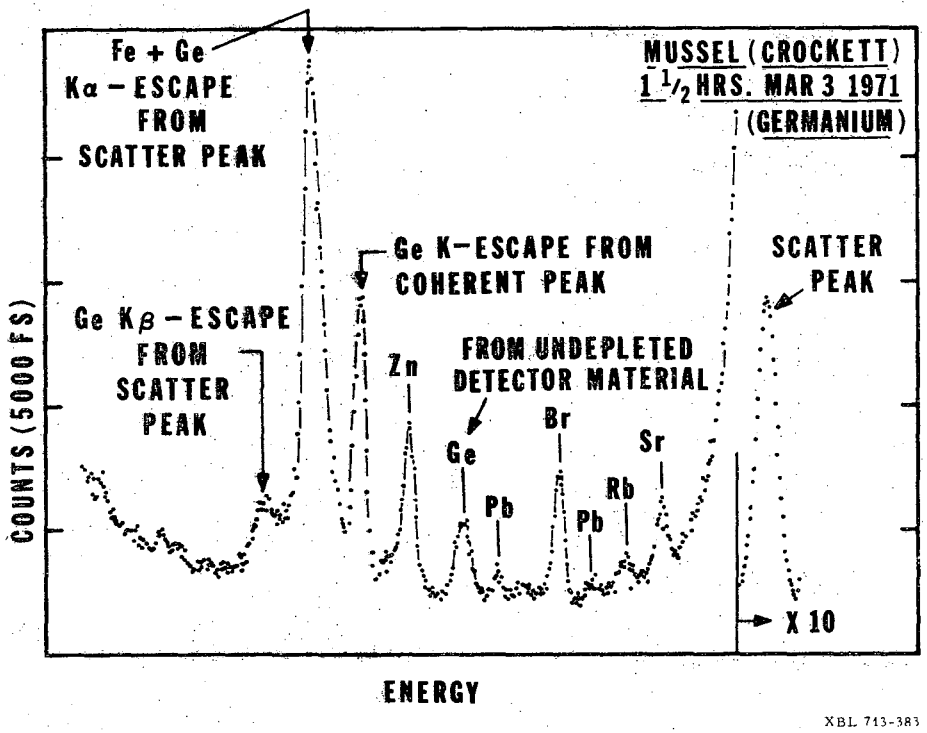

XBL 713-383

Fig. 17. Spectrum obtained with a germanium detector spectrometer on the same sample as Fig. 9. The presence of X-ray escape peaks and germanium X-ray peaks hides much of the real structure in the spectrum.

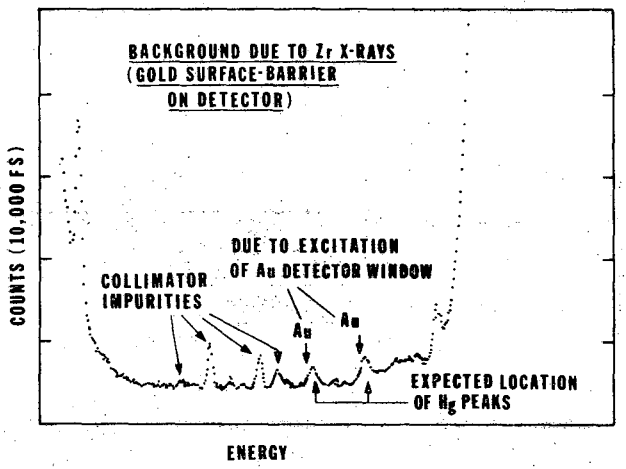

Fig. 18. Spectrum produced by direct irradiation of the detector by Zr X-rays. The effects of the thin gold surface-barrier layer on the detector are clearly shown.

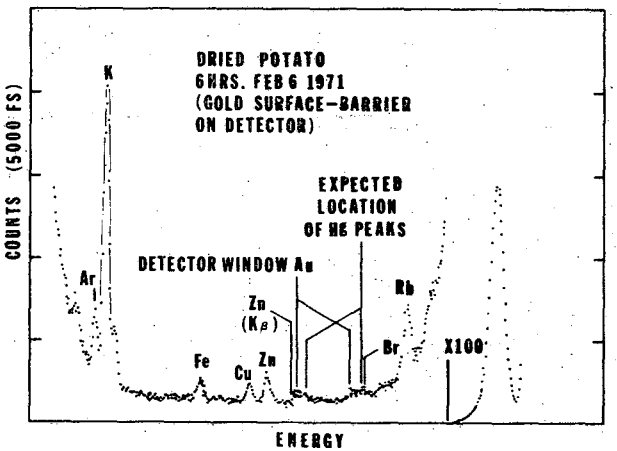

Fig. 19. Spectrum of a dried potato sample showing the confusion produced in the region of mercury lines by the complex lines due to the gold detector window.

the resulting peaks are shifted to the right of the correct location for Au X-rays, and the peak shape is broader than would normally be expected. This phenomena may lead to false identification of mercury in samples. To overcome the problem, materials other than gold must be used to form the surface barrier on the entry side of the detector. It is difficult to achieve non-injecting barriers with other metals, but we have demonstrated that suitable processing can be devised to form nickel or aluminum barriers with suitable characteristics. The remaining results presented in this paper were obtained with detectors having either nickel or aluminum surface barriers at the X-ray entry side.

C. Excitation Sources

So far we have hardly discussed the means used to excite the characteristic X-rays in the sample. In Fig. 1 the source was shown as a ring source and defined no further; later the value of choosing an exciting energy just above the K-shell binding energy of the element of most interest, thereby enhancing sensitivity for this element, was stressed. The ring source used in most experiments is a radioactive source: ^{125}I (producing mostly Te X-rays), ^{109}Cd, and ^{241}Am being the commonest materials used. The high detector background induced by high-energy photons in standard detectors has led to the use of a secondary-fluorescence technique as shown in Fig. 20A; here the sample is shielded from the primary radiation, and is excited instead by the characteristic radiation of a suitable fluorescent

element. In this way, the energy of the backscatter peak from the sample is kept to the minimum required value, and detector background is kept low. Our recent improvements in detector background have made this less important.

Radioactive sources used for excitation suffer from a number of defects. In general, the desired activity is accompanied by contamination of high-energy γ-ray emitting isotopes. High-energy γ-rays that cannot be shielded from the detector produce a general background due to Compton collisions with electrons in the detector. Although this is tolerable in most applications (as witness nearly all the results given here), it does set a lower limit to sensitivity if all other sources of detector background are eliminated.

A more serious problem with radioactive sources is their low intensity. It seems undesirable to propose large-scale use of an instrument containing sources exceeding 100 mC and emitting 4×10^9 photons per sec when, on the other hand, an X-ray tube with only 100 μA flowing in it produces about 10^{12} photons/sec. Since the X-rays are emitted only when required, small X-ray tubes appear less hazardous than large radioactive sources. Furthermore, the anode material can be selected to produce the required excitation energy. Some of the results presented here use radioactive-source excitation, and counting times are measured in hours; using a suitable X-ray tube, we can cut these times to minutes.

The conventional reflection-geometry X-ray tube shown schematically in Fig. 20B emits Bremsstrahlung photons of energies ranging up to the applied voltage, together with the characteristic anode X-rays. If used to directly excite the sample, scatter of the Bremsstrahlung constitutes an intolerable background masking the observation of trace elements in the samples. To avoid this, the X-rays are used to fluoresce a secondary target, whose characteristic radiation then excites the sample. An alternative is to use a small tube as shown in Fig. 20C employing a transmission-type anode in which the thin anode material filters its radiation, transmitting mostly that just below its K absorption edge. The radiation spectrum produced by a tube of this type using a 4-mil Mo anode is shown in Fig. 21. This is almost the ideal spectrum for excitation of a sample. As anticipated, the exciting X-ray intensity is about 100 times that produced by a 100 mC ^{125}I source, cutting down the analysis time accordingly. This is achieved with a power dissipation of only 5 to 10 watts in the anode of the X-ray tube, a level that permits the use of a small structure with good source-sample geometry.

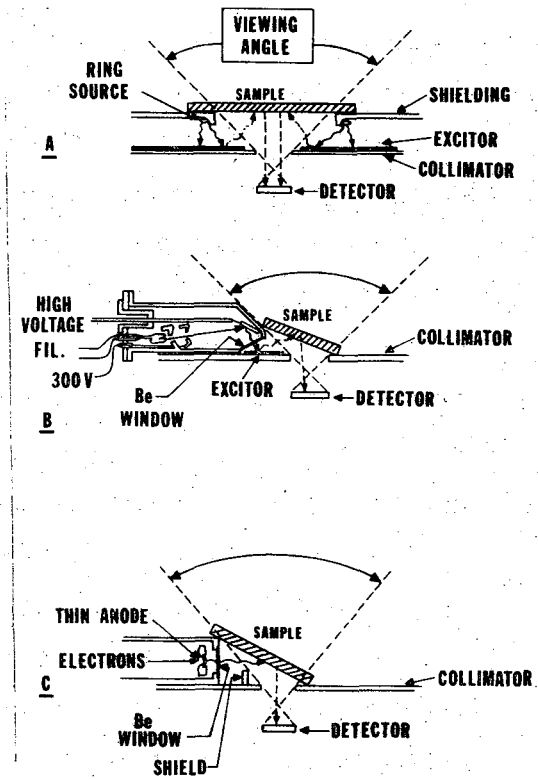

Fig. 20. Three different modes of X-ray excitation in fluorescence spectrometers.

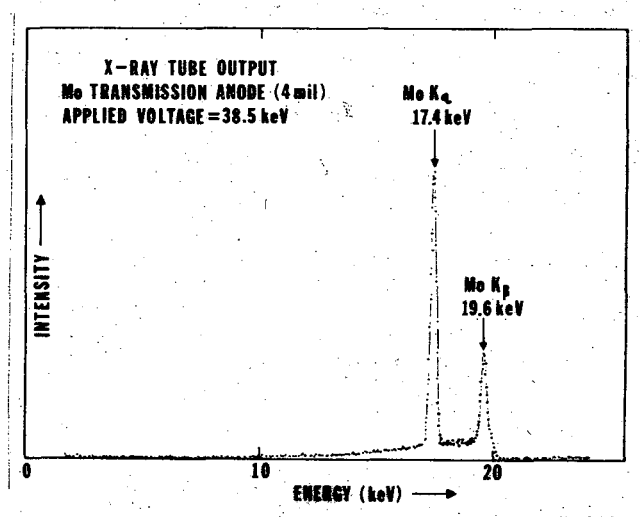

Fig. 21. X-ray output spectrum of a transmission anode X-ray tube (anode material - 4 mil Mo).

BLANK

BLANK

III. EXPERIMENTAL RESULTS AND APPLICATIONS

Semiconductor X-ray spectrometers are distinguished by their ability to simultaneously survey a whole spectrum of trace elements present in samples at levels less than 1 ppm. More sensitive methods can be devised for particular elements: for example, atomic absorption can be used for such elements as mercury. Neutron activation can exhibit greater sensitivity than X-ray fluorescence for some elements; but its sensitivity is poor for many elements, and the activation process is slow and costly. The activation of sodium in biological samples necessitates a long "cooling off" period (often a month) before a sample can be analyzed. Other methods, including atomic absorption, require extensive sample preparation, while X-ray fluorescence requires very little, though removal of water by freeze-drying is useful in many cases. For these reasons, it seems that X-ray fluorescence analysis may find a wide range of applications. A few of these are discussed in this section, and some early results are presented.

A. Analysis of Foods

Public attention has recently been focussed on the adverse effects of certain trace elements in foods. Mercury and cadmium, in particular, have received attention. The toxicity of these elements results from their accumulating in the body and inhibiting important organic functions--this is to be distinguished from the toxicity of chemicals that cause immediate effects on body functions. Furthermore, the

toxicity of an element depends a great deal on its chemical form. In the well-known case of mercury, organic mercury compounds are more toxic than are most of its inorganic salts. X-ray fluorescence gives no information on the chemical form of elements, so it can only be used to flag possible hazards.

Since some trace elements are toxic while others are essential to life, detailed map of trace elements in a wide range of foods should be of value in nutritional studies.

With these points in mind, we will examine a few measurements on foods made with Mo X-ray excitation:*

Figure 22. This test on a freeze-dried tuna sample shows the presence of mercury (~0.5 ppm). However, the sample was concentrated by freeze drying; the original tuna would have assayed at 0.1 ppm of Hg--far below the FDA tolerance (0.5 ppm).

---

* In practice, Mo X-ray excitation restricts the range of elements measured with good sensitivity to the heavy elements (L X-rays), and to the light elements from iron through rubidium. Higher-energy excitation must be used for elements heavier than rubidium. Measurements of elements below iron demand lower-energy excitation, and also the use of thin samples. In both cases, a slight loss of sensitivity will result.

Several features in this spectrum are due to instrumental artifacts. The lead peaks are due mainly to lead contamination of the collimator, while the nickel peak is partly due to the nickel surface-barrier used in this particular detector. These factors are not present in the remaining spectra in this paper. The argon peak is due to excitation of argon present at a level of 1% in the air surrounding the system. We also note that krypton--present to only 1 ppm in air--is observed in some spectra. Helium can be used to displace air when necessary.

A word about calibration is in order at this point. A calibration procedure devised by J. Jaklevic and R. Giauque* uses thin metal layers of known weight to determine geometry factors, excitation efficiency, and sample absorption. This method permits rapid quantiative assessment of the concentrations of impurities observed in spectra.

Figure 23. This test on dried swordfish is to be compared with that on tuna shown in Fig. 22. A very different distribution of elements is seen: iron is almost absent in swordfish, while much more mercury and arsenic are present. Arsenic is probably not a serious problem, but this sample of swordfish (recently purchased) certainly contains more mercury than the FDA limit.

Figure 24. This is liver sausage (freeze-dried). Both mercury and lead are present in higher concentrations than in Fig. 22, but the mercury in this case might well be largely in the form of an

* To be published.

inorganic salt. Although the FDA limit of 0.5 ppm contains no qualification as to chemical form, eating liver sausage might not be a hazardous pursuit!

Figures 25 and 9. These two results demonstrate the wide differences in trace-element distribution in two shellfish. Of particular note is the high concentration of arsenic in the clam, and the high concentration of lead in the mussel. This mussel was obtained in the Sacramento River near an old lead smelter; mussels from other locations contained substantially less lead. The 10 ppm of arsenic in the clam is not surprising; levels as high as 150 ppm have been reported in shellfish from the North Sea off the east coast of England.

B. Plants

Trace elements are known to be an important factor in the growth of plants, and examination of plant material and soils may provide useful information in agriculture. Perhaps the most surprising result of our analysis of plant material has been the high concentration of relatively uncommon elements.

Figure 26 shows the spectrum obtained with a camellia leaf. We show it as a contrast to the other spectra presented here. The large quantities of manganese and strontium were surprising. The ubiquitous lead peak is seen although this particular plant grows far from freeways or city traffic.

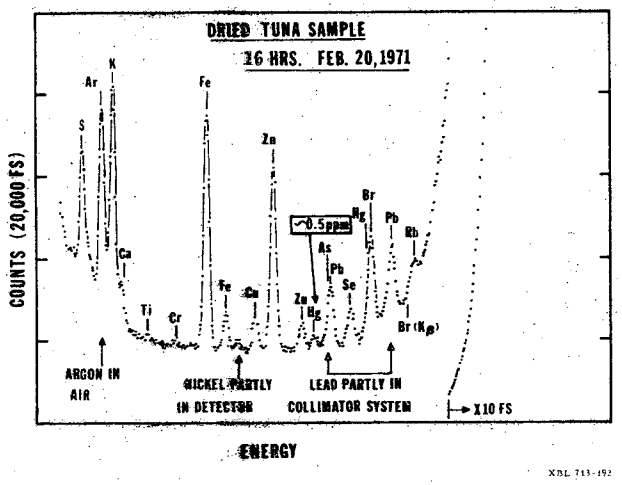

Fig. 22. Dried-tuna spectrum. Features due to the collimator system and other extraneous materials are indicated.

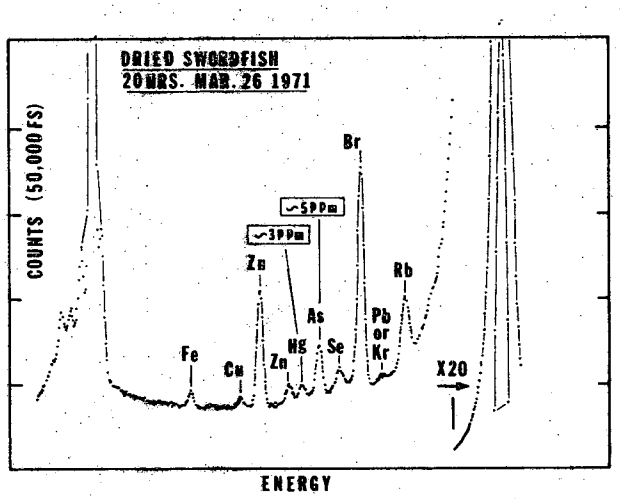

Fig. 23. Dried-swordfish spectrum.

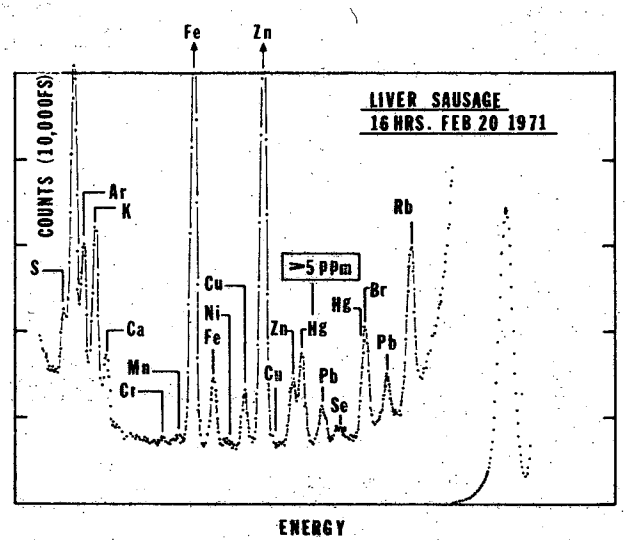

Fig. 24. Liver-sausage spectrum.

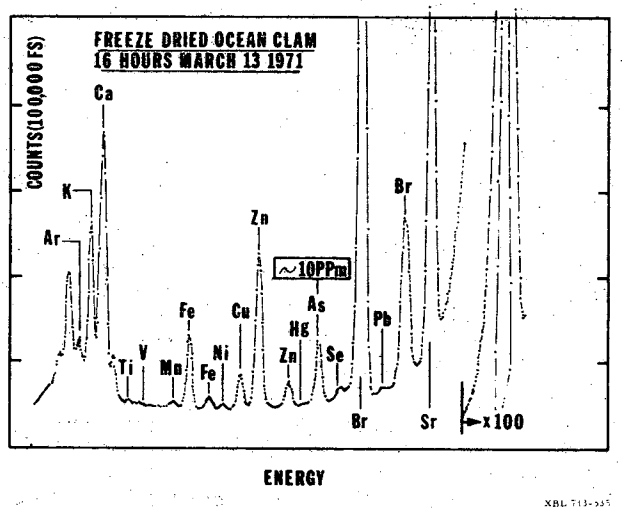

Fig. 25. Dried ocean-clam spectrum.

C. Medical Uses

Medical applications of this technique could turn out to be the most important. Studies[6] have shown that trace elements in blood may correlate with disease states, indicating a possible diagnostic technique. Other readily available samples include urine, hair, fingernails, etc.; the statistical correlations between trace elements in these various samples and disease have hardly been studied at all--mostly due to the lack of a suitable fast, convenient, and accurate method of measurement. Semiconductor detector X-ray fluorescence spectrometers may well stimulate new interest in this field of study.

More specific types of problem also arise in medicine. The examination of organs for trace elements may be an important tool in studying the accumulation of elements in organs and its relationship to diseases, including cancer. One example is the analysis of blood samples for lead, as an indicator of lead poisoning in infants. The X-ray fluorescence method is sensitive enough for this purpose as illustrated in Fig. 27, where lead is clearly determined in a freeze-dried sample (about 3 ml) of normal whole blood. A 0.25-ml sample is adequate for this test, and by using X-ray tube excitation, the measurement time can be reduced to only 15 minutes. Detection of lead at levels indicative of lead poisoning should be a simple matter.

Two other features should be noted in Fig. 27. The large iron peak results in an increase in background at energies below that of the peak. This is due to a small dead layer in this particular

detector. We also note a small peak resulting from escape of silicon K X-rays excited by the iron X-rays. This indicates the care required in interpretation of results, as the escape peak is quite close to the expected location of a vanadium peak (but resolvable by the system).

D. Pollution Studies

Elemental analysis of particulate deposits on air pollution filters presents a simple problem for this technique. With short sample-collection times, the mass of the particulate deposit becomes a substantial fraction of the air-filter material. Consequently, when the filter is subjected to analysis, background due to backscatter in the filter material is quite small. An example of air-filter analysis is shown in Fig. 28. The quantity of lead measured in this sample (from Detroit) corresponds to almost 2 $\mu g/metre^3$ of air, a typical number for air in an industrial area.

Figure 28 also illustrates the use of an X-ray tube to speed up analysis. The transmission-anode tube of Fig. 20C was used to expose the sample for only ten minutes to produce this result--opening up the possibility of on-line analysis of pollution with the capability of seeing fluctuations in particulate pollutants on a time-scale much shorter than an hour.

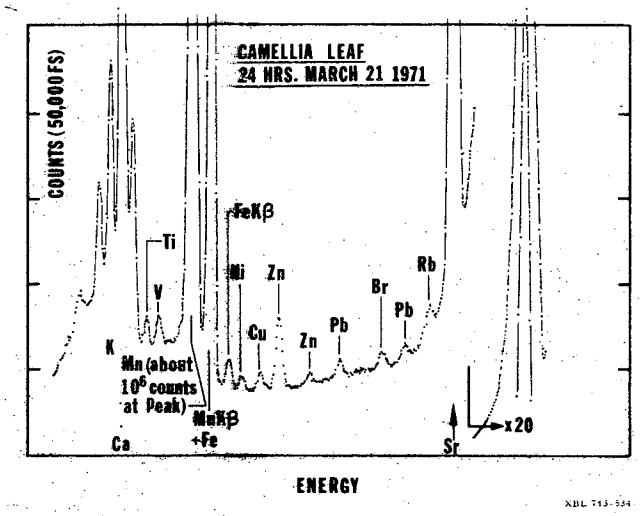

Fig. 26. Camellia-leaf spectrum.

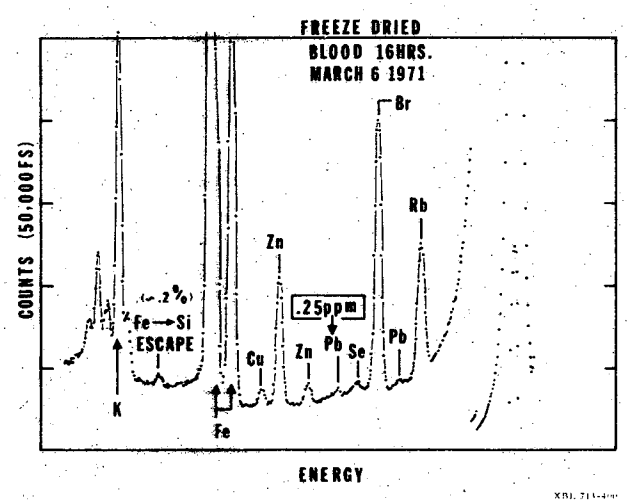

Fig. 27. Freeze-dried whole blood--original blood volume = 3 ml.

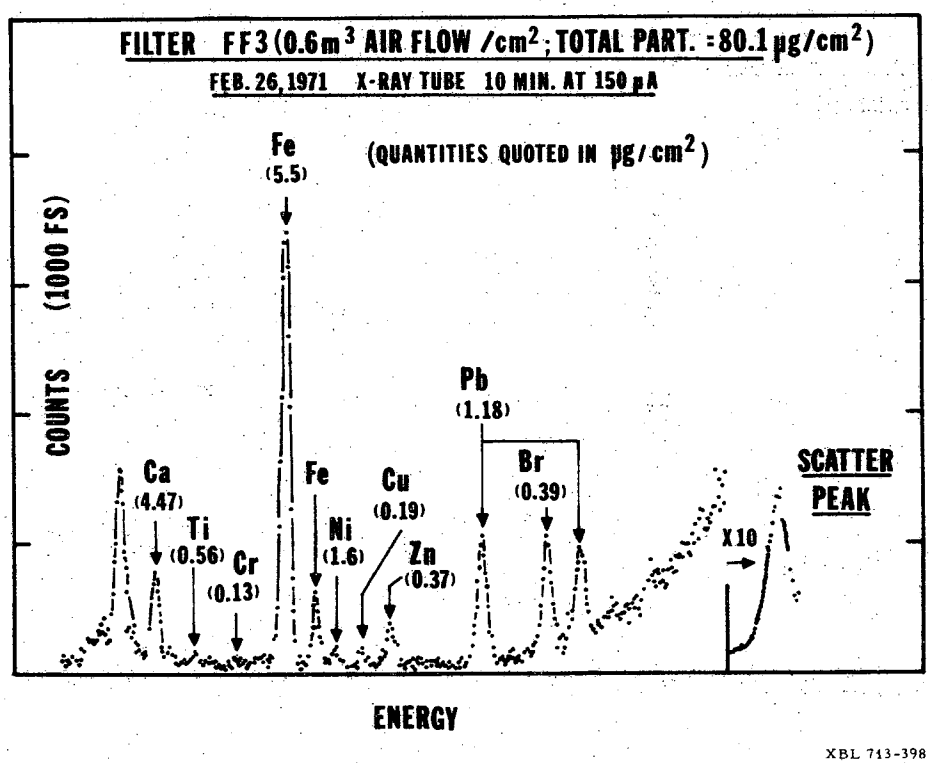

Fig. 28. Air-filter spectrum.

BLANK

BLANK

IV. CONCLUSIONS

The reduction of detector background, improvements in both resolution and counting-rate capabilities of the associated electronics, and the development of a small X-ray excitation source have resulted in an instrument providing an entirely new capability in elemental analysis. High-speed analysis of biological and other samples for a broad range of elements present at levels less than 0.1 ppm can be carried out using X-ray fluorescence. The results presented in this paper are in good agreement with the appropriate sensitivity calculations given in the Appendix. A recent further improvement in detector background is also discussed in the Appendix.

V. ACKNOWLEDGEMENTS

The results given in this paper have depended heavily on the assistance of W. Searles in all phases of the work, on the detector developments of J. Walton and H. Sommer, and on the electronic circuit work of D. Landis, S. Wright and B. Jarrett. D. Malone and J. Anderson have designed and constructed mechanical parts used in the systems. Discussions with R. Pehl, W. Hansen, H. Maccabee, and others, have contributed many ideas to the project. We are particularly indebted to R. Giauque for his persistent interest in the work, for his advice on analytical chemistry aspects of the work, and for demonstrating many of the problems encountered by the user of these systems.

VI. REFERENCES

1. E. Elad, Nucl. Instr. and Methods 37, 327 (1965).
2. H. R. Bowman, E. K. Hyde, S. G. Thompson and R. C. Jared, Science 151, 562 (1966).
3. C. A. Klein, IEEE Trans. Nucl. Sci. NS-15 No. 3, 214 (1968).
4. F. S. Goulding, J. Walton, D. Malone, Nucl. Instr. and Methods 71, 273 (1969).
5. D. A. Landis, F. S. Goulding, R. H. Pehl and J. T. Walton, IEEE Trans. on Nucl. Sci., NS-18, No. 1, 115-124 (1971).
6. J. W. Gofman, Chemical Elements in the Blood in Health, in Advances in Biological and Medical Physics, Vol. 8 (1962) p 1 ed. C. A. Tobias, J. W. Lawrence (Academic) also UCRL-10211 p. 62; Semi-annual Report, Biology and Medicine Donner Laboratory.

APPENDIX

I. GUARD-RING REJECT TECHNIQUE

Recent work has indicated the source of a large part of the background present when the detector guard ring is connected as shown in Fig. 15. Referring to Fig. 29, X-rays entering the detector near the edge of its sensitive region produce a dense cloud of ionization of very small size (~5 microns in diameter). The holes and electrons separate and move toward the appropriate electrodes; in the case shown in Fig. 29, the electrons travel much further than the holes, thereby producing most of the output signal. As the electron cloud moves toward the positive electrode, its size increases due to mutual repulsion of the charges in it--the internal electric fields existing in the cloud far exceed the applied electric field in the detector until the cloud dimensions reach about 100 microns. Consequently, a peripheral region exists at the boundary of the central sensitive region, constituting a fraction

$$\frac{2\pi r}{\pi r^2} \times 10^{-2} = \frac{2 \times 10^{-2}}{r} \quad (8\% \text{ for } r = 0.25 \text{ cm})$$

of the total sensitive volume, from which the charge will be only partially collected in the central region.

To eliminate the background produced by this effect, we detect the guard-ring signal and reject any accompanying signal from the central region, as shown in Fig. 29. In practice, a slightly more

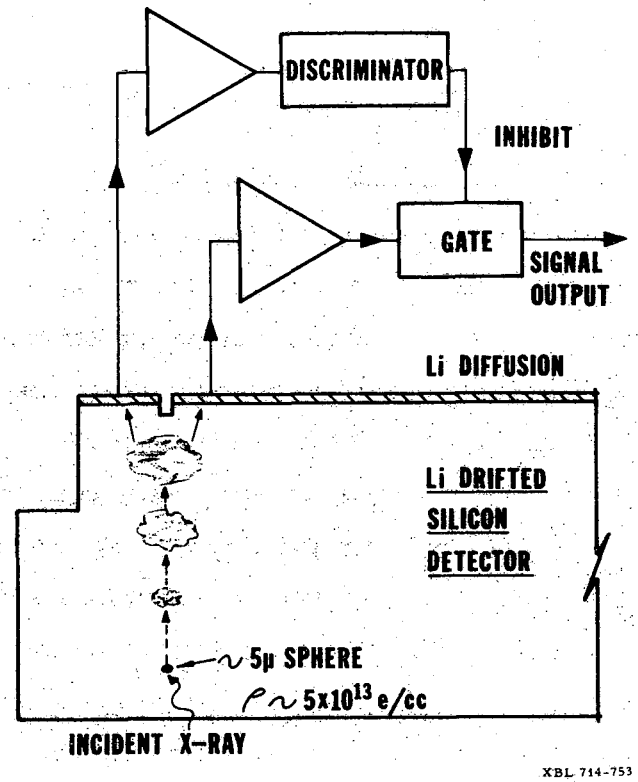

Fig. 29. Guard-ring signal-reject technique used to achieve almost complete background rejection.

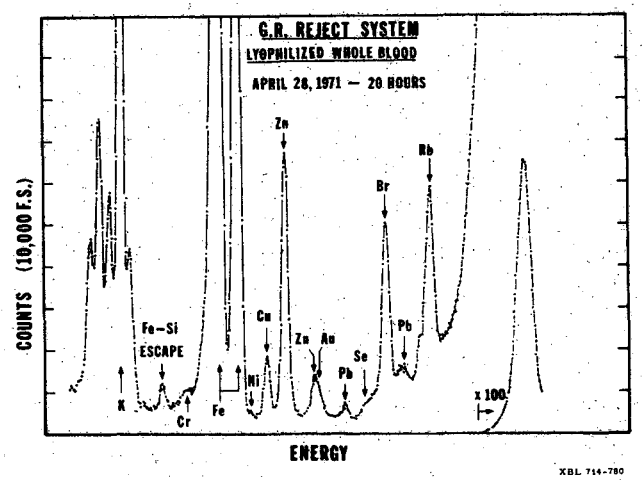

Fig. 30. Freeze-dried blood spectrum produced by final system. This is to be compared with Fig. 27.

complicated arrangement is used, in which a coincidence between guard-ring and central-region signals is required before the main signal is rejected. This requirement reduces the loss of good signals due to accidental coincident counts in the guard ring. Tests have shown that the guard-ring signal-reject system reduces background by a substantial factor compared with the simple guard-ring configuration. The total effect, compared with a conventional detector, is a background-reduction factor of about 50 in typical situations. As an illustration of the improvement achieved by the guard-ring reject system, Fig. 30 shows the spectrum obtained with a guard-ring reject system on the same blood sample as shown in Fig. 27, which was obtained with the simple guard-ring method. A gold surface-barrier was employed on the detector used for Fig. 30; consequently, evidence of gold peaks is seen. The lead peaks due to the < 0.1 ppm of Pb present in normal whole blood are very clearly seen in Fig. 30, while they were only just visible in Fig. 27. Similar improvements in sensitivity have been observed in a number of samples examined with the new system.

II. SENSITIVITY CALCULATION

The following simple calculation of detection sensitivity for lead, using these systems, is in excellent agreement with the experimental results presented in this paper:

For molybdenum Kα radiation:

Total scattering cross-section for an organic matrix = 5 barns/atom.

L-shell photoelectric cross-section for lead $\simeq 3 \times 10^4$ barns/atom.

Fluorescent yield for lead L X-rays = 0.4.

Fraction of L X-rays in Lα peak $\simeq 0.5$.

Effective cross-section for Pb Lα production $\simeq 6 \times 10^3$ barns/atom.

If lead is present at a level of P ppm by weight:

$$\frac{\text{Lead atoms}}{\text{Matrix atoms}} = \frac{0.06P}{10^6}$$

$$\therefore \frac{\text{No. of Pb L}\alpha\text{'s at detector}}{\text{No. of scattered X-rays at detector}} = \frac{6 \times 10^3}{5} \cdot \frac{0.06P}{10^6} = \frac{7.2P}{10^5} \qquad (1)$$

We now suppose that the exciting intensity is adjusted to produce 2×10^4 backscatter counts/sec from the sample, and that a spectrum is accumulated for 1000 sec (16 min.).

$\therefore$ Total counts = 2×10^7.

Peak width for lead Lα line (FWHM) $\simeq 1\%$ of scatter-peak energy.

If X% of scatter-peak counts appear in flat background, the background below FWHM of a Pb peak = 2.10^3 X counts. The RMS fluctuation in this background $\simeq 45\sqrt{X}$.

Assuming that the limit of detection for a peak is twice the RMS background fluctuation, we have:

$$\text{Detectable limit} = 90\sqrt{X} \text{ counts} \qquad (2)$$

for 2×10^7 counts in the scatter peak, equation (1) shows that:

$$\text{No. of Pb L}\alpha\text{'s at detector} = 1440\ P. \qquad (3)$$

Combining (2) and (3), we have:

$$P_{LIM} = \frac{90}{1440}\sqrt{X} = \underline{\underline{.06\sqrt{X}}}\ .$$

The following sensitivities should therefore apply to our detector systems: X = 6% (simple guard ring); P_{LIM} = 0.15 ppm

X = 0.6% (guard-ring reject); P_{LIM} = 0.05 ppm

(These results are achieved in about 15 minutes using X-ray-tube excitation.)

LAWRENCE BERKELEY LABORATORY

UNIVERSITY OF CALIFORNIA

BERKELEY